

## **Retraction Notice**

The Editor-in-Chief and the publisher have retracted this article, which was submitted as part of a guest-edited special section. An investigation uncovered evidence of systematic manipulation of the publication process, including compromised peer review. The Editor and publisher no longer have confidence in the results and conclusions of the article.

KL, LX, DZ, and JX either did not respond directly or could not be reached.

# Application of remote sensing image ecological land classification method in crop planting area extraction under the background of data fusion

Kexue Liu,<sup>a</sup> Lingyu Xia,<sup>a</sup> Dongya Zhu,<sup>b</sup> and Jianbo Xu<sup>c,\*</sup>

<sup>a</sup>Guangzhou Xinhua University, Department of Resources and the Urban Planning, Guangzhou, Guangdong, China

<sup>b</sup>Guangdong Dongtu Planning Technology Co., Ltd., Guangzhou, Guangdong, China

<sup>c</sup>South China Agricultural University, College of Resource and Environment, Guangzhou, Guangdong, China

**Abstract.** Data mining is a common basic function in humans and many other intellectual systems. The popularization of computers has created a good research environment for the advanced application of remote sensing satellites. With China's economic and population growth, the demand for food is also increasing. Obtaining the planting area is one of the most important tasks in calculating harvest costs. However, traditional cost analysis methods lack information. The traditional remote sensing image classification method is based on the pixel classification method, which cannot effectively extract the spatial texture information in an image. The pixel-based classification method also has the problem of salt and pepper phenomenon in the classification results, which generates a large number of invalid broken patches and ultimately leads to low classification accuracy. Here, we investigated the application of remote state system mapping for the extraction of the planting area. We analyzed the basic principles of remote image processing and remote image sharing methods and introduced an audio system and optical algorithm. Here, two separation methods are selected, long-distance traction measurements are performed in three training areas, and the two results are compared and analyzed. Experimental results show that the method of objective orientation increases the working speed compared with the method of manuscript translation. The benefit of speed measurement becomes more apparent in both seasons as the measuring range increases. Computer automatic classification and the method of artificial visual interpretation are tested sequentially, and the total time taken is 49 and 13.5 days, respectively. © 2022 SPIE and IS&T [DOI: [10.1117/1.JEI.31.5.051407](https://doi.org/10.1117/1.JEI.31.5.051407)]

**Keywords:** remote sensing image; land classification; remote sensing measurement; crop area; object-oriented classification.

Paper 210818SS received Dec. 22, 2021; accepted for publication Mar. 14, 2022; published online Apr. 21, 2022.

## 1 Introduction

Effective measures must be taken to ensure food security and stabilize food production. To cope with the food security crisis, China has adopted a subsidy policy of fine seeds, i.e., to provide farmers in a region with dominant species promoted by the country and give them certain financial subsidies according to different varieties. The purpose is to increase farmers' enthusiasm for planting dominant species, increase the coverage of fine seeds, increase yield, stabilize the total output of grain cultivation, and promote the pace of agricultural modernization. With the continuous improvement of the resolution of remote sensing images, people are becoming more and more proficient at making full use of high-resolution remote sensing images.

With the development of science and technology, the performance of sensors has been greatly improved, and a large number of multisensor systems for complex application backgrounds has emerged. The rapid development of industrial production technology and the continuous

---

\*Address all correspondence to Jianbo Xu, [xujianbo@scau.edu.cn](mailto:xujianbo@scau.edu.cn)

precision of the output process are inseparable from environmental measurement and control. The development of technology has allowed for the object to be measured and controlled to be more and more complex. It is difficult for a single isolated sensor to control the complex object to be measured. Whether it is comprehensive information or some inherent characteristic information, it is difficult to guarantee the accuracy and precision of the information obtained by itself. In addition to understanding the measured size of the measured object, it also needs to meet the more accurate measurement and control requirements. In those days, domestic research on information fusion technology was carried out late due to the limitation of economic level and scientific research conditions. In recent years, researchers have conducted exploratory research on remote sensing classification methods from the perspective of image segmentation units or patches and have made some progress. These methods are the prototype of object-oriented classification methods. The need for rich ground information and texture information for crop information extraction is also increasing. At present, the research on crop area measurement using remote sensing technology is mainly focused on foreign satellite data, which is relatively expensive. Making good use of domestic satellites for crop area measurement is becoming more and more important. Another concern is the effective use of remote sensing data. When using remote sensing images for crop area measurement, multitemporal high-resolution remote sensing image data can be used to obtain crop planting areas that meet the accuracy requirements, providing real-time or quality-compliant data according to established research requirements. So, with limited data, it is necessary to further study whether high-precision crop area measurement can be performed. In response to the above problems, this paper attempts to select a single-phase domestic high-resolution remote sensing image data method based on multiple periods of remote sensing data and phenological data and uses field sampling survey data to be true values. Two methods, visual measurement and object-oriented information extraction, are used for comparison experiments of crop area measurement to obtain an effective method for large-scale and rapid extraction of crops. Compared with human visual interpretation, computer interpretation has a high status and can quickly obtain various thematic information on the surface, which greatly reduces the workload and interpretation time of image processing and improves work efficiency. However, the existing computer-aided information extraction methods to classify remote sensing images mostly use traditional pixel-based classification methods, which only use the spectral information of the pixels. However, the interdependence between adjacent pixels and a large amount of spatial information of remote sensing is ignored. The integration and complementation of various remote sensing information sources are basically not considered, the obtained result information is very limited, and there are often many broken and invalid patches in the results, which seriously affects the classification accuracy and information extraction accuracy.

Gong et al. believed that customizing the remote projection function plays an important role in many applications, so it has received a great deal of attention. In recent years, great efforts have been made to develop more data systems or to propose more methods for position adjustment from remote sensing images. However, a systematic review of the literature on datasets and event customization methods is also available. In addition, almost all existing data sets have a number of limitations, such as the small size of the event categories and the number of images, the lack of contrast and image contrast, and the satisfaction of accuracy. These limitations hinder the development of new methods, especially those based on in-depth learning. They start with a comprehensive overview of new developments. Northwestern Polytechnical University created large data system called Northwestern Polytechnical University (NWPU)-RESISC45, which is an open-source platform for remote visual imaging (RESISC). The documentary contains 31,500 images covering 45 categories of events with 700 images in each category. In terms of event categories and a total number of images, the proposed NWPU-RESISC45 is extensive. There are significant differences in meaning, spatial resolution, visual acuity, sound stability, lighting, formation, and movement with a high variety in the class and similarity between classes. This dataset will allow the community to develop and compute many data management algorithms. Finally, several representative methods were calculated using the proposed data set, and the results were reported as useful criteria for future research.<sup>1</sup> Karalas et al. believed that analog signage was expensive and required a lot of work, so obtaining high-quality landfill was a difficult task. This project introduces a whole new approach to this area by expanding the use of

remote satellite imagery, which can produce new land cover maps. They proposed a robust multi-tagging process in machine learning to determine the relative relationship between recorded satellite images and the rotations of different types of surface materials. Compared with the prognosis of unhealed wounds, Karalas et al. developed a completely different approach. As part of the isolation monitoring process, Karalas et al. used data collected on the basis of the European Environment Agency to develop a set of symbols and generated multiple images from the MODIS sensor to produce spectral characteristics. To confirm the benefits of their approach, they formulated results using multiple multibrand training units and calculated their predictive performance against certain defined training models and the ability to handle project examples from local communities or communities. They also introduced the application of their approach to Hyperland sensor data for ground cover analysis in New York. Even with a limited number of different training models, the proposed procedure can achieve optimal prognostic accuracy and, therefore, go beyond the new methods of vision impairment.<sup>2</sup> Su et al. believed that the use of remote widgets to monitor land use and land cover changes is necessary to assess the impact of human activities on the environment. Finding a digital transformation can help determine the potential of landscape transitions. They found that, compared with pixel-based customization, material adaptation was effective in generating ground cover information and changing its timing. Landsat images from the two-season series (1990 and 2015) were used to analyze the spatio-temporal rotations of different types of land cover in the Vientiane region of the Lao People's Democratic Republic. They used the top-down method to sort Landsat images into three sliding steps with improvement steps. Use scales of 25, 10, and 5 (with different weight scales) were used to designate different types of land cover in Vientiane in 1990 and 2015. Through the adjustment, the total land cover balance and kappa numbers increased by 13.44% and 0.16, respectively (LCC1990). For LCC 2015, overall accuracy (OA) and kappa ratios improved by 28.71% and 0.25, respectively.<sup>3</sup>

This paper first analyzes the basic principles of remote sensing image processing and remote sensing image segmentation methods and then introduces the process of two classification algorithms of object-oriented computer automatic classification and manual visual interpretation. In the experimental part, these two classification methods were selected, crop remote sensing measurements were carried out in three study areas, and the two measurement results were compared and analyzed. We researched and explored the classification technology of object-oriented multi-source remote sensing data comprehensive utilization. Using object-oriented multisource remote sensing image analysis technology, comprehensively using multisource remote sensing data, and giving full play to the advantages of different remote sensing data, we realize rapid and intelligent identification of remote sensing information and high-precision information extraction through fuzzy logic reasoning and other methods. Reliable, comprehensive, and accurate target remote sensing information can be efficiently extracted from the data.

## 2 Proposed Method

### 2.1 Remote Sensing Image Data Processing

Remote sensing image data processing is a technical means to perform radiometric correction and geometric correction, image trimming, projection transformation, mosaic, feature extraction, classification and various thematic processing operations on remote sensing images.

#### 2.1.1 Basic principles of remote sensing image extraction

Image segmentation is an object-oriented recognition and analysis technology based on the characteristics of image information itself. Image segmentation is actually the division of content into regions, and an image is divided into several sub-regions with distinct characteristics.<sup>4,5</sup> Image classification classifies the information with common attributes or characteristics inside these subregions and between the subregions and adjacent regions, and it detects some feature information in the images at the same time. Image extraction is based on the results of classification processing to extract the target object. The biggest difference is that the extraction is actually the

image input for classification results, and the segmentation technology is the area of the image before classification.<sup>6,7</sup> For object-oriented image processing methods, successful image segmentation is a necessary premise, and the segmentation results will directly affect the accuracy of the classification results. Therefore, image segmentation is a crucial step in object-oriented classification methods.

Suppose that the object in an image  $p(x, y)$  is divided into several sub-images  $p_1, p_2, \dots, p_n$ , and the result of the segmentation needs to satisfy the following definitions:

1.  $\bigcup_j^N p_j(x, y) = p(x, y)$ ; this formula requires that each pixel in the image is completely segmented into sub-regions.
2.  $p_j(x, y) \cap p_i(x, y) = \mu$ , for  $\forall j, i, i \neq j$ ; this formula shows that each subregion is not related to each other.
3. It is necessary to keep the difference of pixels in the same area to a minimum, and the change is not large.

Through machine vision, the position, structure, distribution characteristics, and size of the same type of features are determined, processed, calculated, and analyzed according to the spectral characteristics and spatial characteristics of the remotely sensed images to achieve automatic classification of the images. The spatial characteristics of the whole area are divided into countless subareas, and each subarea represents the actual category of ground objects, thereby extracting the target object.<sup>8,9</sup>

### 2.1.2 Common methods for remote sensing image segmentation

Image segmentation is a key step in extracting target objects, and the accuracy of the segmentation method is increasing. Researchers have proposed various segmentation algorithms for the large size and rich content of remote sensing images. This article mainly introduces the clustering methods involved in the paper: the expectation-maximization (EM) algorithm and the kernel fuzzy  $c$ -means (KFCM) algorithm.

**Expectation-maximization algorithm.** The EM algorithm is a simple and practical method. It is actually an incomplete data set, and then uses the estimation result as the basis of the sample to perform maximum likelihood estimation on the data of the entire sample space. It is used to estimate the sample model parameters in image information, and it is also an effective clustering method.<sup>10,11</sup> When the sample distribution in the image information belongs to a certain model, the EM algorithm first estimates each of its parameters and then combines the given original data to complete the clustering process. The information is classified into different distributions based on the maximum likelihood probability of each sample.<sup>12,13</sup> The vectorized data, such as the elevation assignment, are further processed to generate an EM model, i.e., a digital elevation model. EM is important basic data for geographic information system (GIS) analysis and processing. It can store elevation data of the digital terrain, display three-dimensional (3D) ground landscape, and extract terrain factors such as slope and aspect. It has important reference values for remote sensing image analysis and information extraction.

Step 1: In the model space, give an initial value  $A_0$ ,  $k = 0$  according to the parameter estimation.

Step 2: Calculate the auxiliary function from the given estimated value  $A$

$$Q^N(A, A_k) = E(\log L(A|x, z)) = \int_z \log p(x, z|A) f(z|x, A_k) dz. \quad (1)$$

Step 3: To get  $Q^N(A, A_k)$  maximization, there must be  $Q^N(A_{k+1}, A_k) = \max(A, A_k)$  in the space.

Step 4: If  $\log L(A_{k+1}) - \log L(A_k) \leq \varepsilon_1$  or  $\|A_{k+1}, A_k\| \leq \varepsilon_2$ , the iteration is aborted; otherwise  $k \leftarrow k + 1$ , and return to step 2.

**Fuzzy cognitive map algorithm.** The fuzzy cognitive map (FCM) algorithm builds an iterative process based on the sample data set by changing the squared error within the class

into a weighted sum of squared error within the class. The EM algorithm not only provides a basis for remote sensing image interpretation, image control point selection, training sample area determination, and interpretation accuracy analysis but also, through spatial analysis and processing, obtains important knowledge and rule models for remote sensing image information extraction, so as to achieve the purpose of improving the classification accuracy of composite remote sensing images.

The objective function is

$$J(u, v) = \sum_{i=1}^c \sum_{k=1}^N u_{ik}^2 d^2(x_k, v_i). \quad (2)$$

According to the definition of the objective function of the FCM algorithm, the pixel values of the image can be regarded as a data set  $X = \{x_1, x_2, \dots, x_N\}, x_k \in R^d$  with  $N$  samples, and the  $N$  pixel values are divided into  $c$  cluster centers ( $2 < c < 1$ ). From Eq. (2), it can be seen that  $u$  represents the degree of membership of the  $k$ 'th sample belonging to the  $i$ 'th cluster center,  $v$  represents the cluster center matrix, and  $d^2(x_k, v_i) = \|x_k - v_i\|^2$  in the expression is a sample data point  $x_k$  to the cluster center  $v_i$ .

Classify the samples in different remote sensing image information, get different classification results to form a subset of samples, and generate corresponding objective function  $J(u, v)$  values. To obtain the best effect of clustering, then the value of  $J(u, v)$  must be minimized, and each column of  $u_{ik}$  must be unconnected. The criterion for clustering based on the objective function is

$$\min J_m(u, v) = \min \left\{ \sum_{i=1}^c \sum_{k=1}^N u_{ik}^m d^2(x_k, v_i) \right\}. \quad (3)$$

Let  $\sum_{i=1}^c u_{ik} = 1$  calculate the membership  $u$  and the clustering center matrix  $v$  according to the Lagrangian multiplication calculation rule, which is obtained by combining with Eq. (3)

$$F = \sum_{i=1}^c \sum_{k=1}^N u_{ik}^m d^2(x_k, v_i) + \sum_{k=1}^N \lambda_k \left( 1 - \sum_{i=1}^c u_{ik} \right). \quad (4)$$

Step 1: Determine the initial values of the parameters  $c$  and  $m$  according to the objective function, and give the conditions for the algorithm to stop iteratively.

Step 2: Calculate membership matrix

$$u_{ik}^{(t)} = \frac{d(x_k, v_i)^{-2/(m-1)}}{\sum_{j=1}^c d(x_k, v_j)^{-2/(m-1)}}. \quad (5)$$

Step 3: Update the cluster center

$$v_i^{(t+1)} = \frac{\sum_{k=1}^N [u_{ik}^t]^m x_k}{\sum_{k=1}^N [u_{ik}^t]^m}. \quad (6)$$

Step 4: Set the maximum number of iterations  $T$  after the update, and determine whether the iteration condition  $\|v_i^{t+1} - v_i^{(t)}\| < \epsilon$  is reached. When the condition is reached, the iteration stops; otherwise let  $t = t + 1$ , return to step 2 to calculate the membership and update the cluster center.

**Kernel fuzzy c-means algorithm.** KFCM is also known as the fuzzy  $c$ -mean algorithm based on the kernel function. It mainly replaces the Euclidean distance in the traditional FCM algorithm with the kernel function. Thus, the degree of difference between categories is increased, and the classical FCM does not easily deal with fuzzy categories.

The KFCM algorithm actually introduces a kernel function based on the FCM algorithm. Assuming that the spatial sample set is  $X = \{x_1, x_2, \dots, x_N\}$ ,  $x_k \in R^d$ ,  $j = 1, 2, \dots, N$ , define  $\Phi$  to perform nonlinear mapping of the data to complete the algorithm implementation process, and use  $K(x, y)$  to represent the mapped space expressed as  $K(x, y) \leq \Phi(x) - \Phi(y) \geq \Phi(x)^T \Phi(y)$

$$\|\Phi(x) - \Phi(y)\|^2 = (\Phi(x) - \Phi(y))^T (\Phi(x) - \Phi(y)) = K(x, x) + K(y, y) - 2K(x, y). \quad (7)$$

If a Gaussian kernel function is selected,  $K(x, x) = K(y, y) = 1$ , then

$$\|\Phi(x) - \Phi(y)\|^2 = 2 - 2K(x, y). \quad (8)$$

The objective function of KFCM is

$$J_m = \sum_{i=1}^c \sum_{k=1}^N u_{ik}^m \|\Phi(x_k) - \Phi(v_i)\|^2 = 2 \sum_{i=1}^c \sum_{k=1}^N u_{ik}^m [1 - K(x_k - v_i)]. \quad (9)$$

The membership function is as follows:

$$u_{ik} = \frac{\frac{1}{[k(x_i, x_k) - 2k(x_k, v_i) + k(x_k, v_i)]^{\frac{1}{m-1}}}}{\sum_{j=1}^c \frac{1}{[k(x_i, x_k) - 2k(x_k, v_j) + k(x_k, v_j)]^{\frac{1}{m-1}}}} = \frac{[1 - k(x_k, v_i)]^{-\frac{1}{m-1}}}{\sum_{j=1}^c [1 - k(x_k, v_j)]^{-\frac{1}{m-1}}}. \quad (10)$$

The cluster center function is as follows:

$$v_j = \frac{\sum_{k=1}^N u_{ik}^m K(x_k, v_i) x_k}{\sum_{k=1}^N u_{ik} K(x_k, v_i)}. \quad (11)$$

When  $\|v_i^{t+1} - v_i^{(t)}\| < \epsilon$ , stop the iteration process; otherwise return to continue to calculate the membership function, update the cluster center, and output it if the iteration stop condition is reached.

## 2.2 Ecological Taxonomy

### 2.2.1 Basic characteristics of ecological classification

Ecological taxonomy has the following basic characteristics:

1. Ecological classification has the basic characteristics of traditional image classification.
2. The ecological taxonomy is basically carried out on the basis of complete administrative divisions, which is convenient for comparative analysis with socio-economic data.
3. Geographical division divides regions with large differences, small similarities, small differences, and large similarities within regions. Image processing for each sub-region is beneficial for reducing the influence of the same-spectrum foreign body or the foreign-spectrum appearance.

### 2.2.2 Essence of ecological classification

The essence of the ecological classification method for extracting crop area information is based on the following considerations:

1. The natural environment in the region is relatively consistent, and there are certain differences between regions. The elements of the natural environment considered are the consistency and diversity of the landform, soil, climate, hydrology, and plant distribution and their interaction. Zoning is based on the natural environment background of crop

growth to achieve the consistency of the natural environment and inter-regional differences of crop growth in the region.

2. There must be consistency of crop growth characteristics and regional differences. This mainly reflects the image characteristics and image classification requirements of corn, the growing process of the object that we classify. For example, due to the different growth periods of different varieties of corn, late-maturing varieties are in the maturity period in early September. This phase image can be used to extract corn area information. At this time, early maturing varieties are in the harvesting period, and it is no longer suitable for extracting corn area information.

### **2.3 Object-oriented Computer Automatic Classification and Data Fusion Technology**

#### **2.3.1 Object-oriented crop area measurement method**

This study is based on the processed four band orthophoto results, using the multiscale segmentation rule to perform the initial segmentation of the image and then training these polygon selection samples to establish a classification rule system. The standardized nearest neighbor classification method is used for each study area. The extraction of crop information and non-crop information and, in the ArcGIS software platform, the manual modification and improvement allow for obtaining more accurate remote sensing measurement results of crop areas. Due to the salt and pepper effect of the pixel-based classification method, a large number of broken patches appear after converting to vector data, which needs to be processed by removing small patches, but the process of removing small patches can only consider the largest patch adjacent to it. Instead of considering the merging of patches with the closest spectral values, the final terrestrial boundaries do not match well enough. In the process of image segmentation, the object-oriented classification method generates image objects with the smallest difference in internal homogeneity, so the boundary of the object is highly consistent with the boundary of the land type. The pixel-based classification method must undergo post-classification post-processing with GIS participation, such as re-visual interpretation of roads, rivers, etc. and manual vectorization modification. The misclassification of various land types also requires certain modifications, which is a cumbersome process, and cannot improve accuracy effectively.

#### **2.3.2 Image segmentation**

**Determination of multiscale segmentation parameters.** Multiscale segmentation parameters mainly include band weights, segmentation scales, and homogeneity factors, which include spectral factors and shape factors. To get a satisfactory segmentation result, the setting of each parameter is very important. Multiscale segmentation technology can construct image object layers at different representation scales for the same image, and there is a certain topological relationship between each object layer. This provides a guarantee for the selection of the best scale for thematic image classification. There is a strict sequential inheritance between the object layers, the boundaries of the objects between the upper and lower layers are consistent, each layer object is built on the basis of its next layer object, and the area of the upper layer object is all of the objects in the lower layer corresponding to it, or the sum of the regions.

The choice of band weight is one of the important factors affecting the segmentation effect. The weight values of different bands are mainly set according to the importance and suitability of the band in the image segmentation process. Generally, a larger weight can be given to a band that contains more image information or a band that is more useful for extracting a certain type of thematic information at present, while a less important band can be left unpartitioned or given a smaller weight.

The segmentation scale is an abstract term without a clear unit. It is a threshold for measuring the heterogeneity of two adjacent image objects. The segmentation scale is an important parameter for image segmentation. Its selection determines the size, number, and information extraction of the segmented objects. Accuracy, that is, whether an ideal image segmentation result can be obtained, depends on whether the selected segmentation scale is appropriate.

The homogeneity factor is used to represent the smallest heterogeneity, including the spectral (color) factor and the shape factor, and the sum of their weights is 1. In general, the proportion of the spectral factor and the shape factor is dominated by the spectral factor, that is, set to about 0.8/0.2. If the shape of the ground type in the image can truly reflect its characteristics, the proportion of the shape factor can be appropriately increased while decreasing the specific gravity of the spectral factor.

**Automatic classification.** eCognition software provides a variety of information extraction methods, including nearest neighbor classification, membership function classification, decision tree classification, and thresholding. Due to the large differences in ground features in the study area and the difficulty in separating similar classes with an object feature, this study uses the nearest neighbor classification method for object-oriented information extraction.

The selection and definition of feature space are crucial for object-oriented information extraction. In automatic classification, you need to select appropriate features according to your needs and construct feature functions to define the feature space of each class. When defining feature space, you can define only one type of feature or multiple features. However, it should be noted that the more features that are involved in classification, the higher the classification accuracy is. When multiple features are combined with each other, different features will also affect each other. If redundant features appear, it will not only increase the calculations amount but also reduce the classification efficiency and even reduce the classification accuracy. Therefore, for specific types of features, you do not need to define too many non-obvious features; you only need to selectively define the most obvious features.

The recognition software provides a large number of remote sensing image features, including target features, related features, and global image features. Among them, the target features mainly refer to the spectral heterogeneity, shape difference, and texture difference between the image objects after segmentation; the related features are mainly used to describe the subordinate relationship between the image objects; and the global image feature refers to the entire scene image or view inside the image scale information. Common characteristics include:

Spectral features are the most direct source of information for remote sensing images. They are inherent features of ground features and are the basis of shape and texture features. The spectral characteristics mainly include mean, standard deviation, ratio, and brightness.

Shape features refer to the differences in image shapes based on the shape and contour of the feature. Shape characteristics mainly include length, area, aspect ratio, shape index, and compactness.

The texture feature is one of the spatial features of the image that better considers both the macro and fine structures of the image. The texture features mainly include the homogeneity index, contrast of the gray-level co-occurrence matrix, and the information entropy of the gray gradient vector grey-level co-occurrence matrix. In addition, users can customize some feature functions according to actual needs to improve classification accuracy. Common custom feature functions include:

Normalized differential water index (NDVI)

$$NDVI = (NIR - R)/(NIR + R). \quad (12)$$

Normalized differential vegetation index (NDWI)

$$NDWI = (G - NIR)/(NIR + G). \quad (13)$$

Before defining the feature space, aiming at the study area classification system and research focus, we learned the basic characteristics of each major land type from the research in other scholars' related fields:

The basic characteristics of vegetation include crops, forest grassland, horticultural fruit trees, and other places. The reflection characteristics of the spectrum are strong, especially in the near-infrared and red bands, which show strong reflection and absorption characteristics. Area woodland texture is generally more uniform and smoother; crops and horticultural fruit trees are generally more regular in shape, whereas forest grasslands are less regular. Generally, NDVI, entropy in the texture eigenvalues, and variance are used to construct the index

information of the vegetation. The shape features can also be used to extract green forest land, green grass, and crops.

The reflection characteristics of waters are mainly manifested in the blue wave band. Among them, static waters, in addition to the blue wave band, also perform prominently in the green wave band; for flowing waters, there are strong absorption characteristics in the green wave band and the near-infrared wave band. Waters are generally not regular in shape. Normally, the normalized difference water body index NDWI is selected to construct the index information of the water area; the water area information can also be extracted by the characteristics of the blue band ratio value and the standard deviation.

The geometric features and gray values of roads are obvious, especially on high-resolution images. Generally, features such as aspect ratio, gray average, asymmetry, NDVI, and density are used to construct road index information.

The land for construction, especially the land for houses, is relatively regular. The internal gray value is relatively uniform, and the boundary is relatively large compared with the surrounding features.

Other land mainly refers to desert and bare land. Generally, it has high reflection, high brightness, and clear texture on high-resolution images.

In the actual data fusion system, the data reported by the sensor cannot be simply transmitted to the fusion center. When each sensor reports the data, it is necessary to add the time stamp and the sensor's own working status information for the system to identify it for fusion processing. In a multisensor target tracking system, the system's state equation is usually described by rectangular coordinates, and various sensors report data based on their own spherical coordinate system, so the system's observation equation is a nonlinear state equation. The parameter estimation problem of the single-sensor system is transformed into the parameter estimation problem of the multisensor system. After the data are collected, they are preprocessed before the data fusion operation to eliminate errors, thereby improving the accuracy of the experimental results. It is also a functional part of the data fusion

$$\delta_o = (\alpha_i(x)) = \sum_{i=1}^x H[h_i(x) | y^h] \beta h_i(x), \quad (14)$$

$$A_1(h|h) = A_1(h|h-1) + H_i(h) s_i(h), \quad (15)$$

$$S_i = \sqrt{(h=1)} \sum_{i=1}^a \beta_{i-1}(h) S_{i0}(a-1). \quad (16)$$

Among them,  $A_1(h|h)$  calculates the correlation probability between attribute  $\beta$ , and  $H$  represents the state. We predicted the status update of the measurement target  $i$   $\delta_o$ .

## 2.4 Manual Visual Interpretation

### 2.4.1 Establishing interpretation marks and measurement templates

Before performing crop remote sensing measurements, we first correlate based on the spectral features, geometric features, texture features, imaging time, and ground features of the image, combined with the socioeconomic conditions of the study area and field survey data, through classification and comparison methods, such as reasoning and comprehensive analysis. Experienced professionals in image interpretation analysis and research understand platforms, remote sensors, imaging methods, including imaging date, season, area range, image scale, spatial resolution, and color synthesis scheme. In this study, we focus on analysis of spectral, spatial, and temporal characteristics; various types of ground features; analysis of location, size, geometry, color, hue, contrast, and shadow; and other characteristic information on different types of land, with the establishment of nine lands in each. A similar interpretation of the study area is to lay the technical foundation for remote sensing measurement of the crop planting area, which is in operation, supplement, and improvement.

### 2.4.2 Determination of land type

Common methods of visual interpretation include empirical methods, peripheral inference methods, and data-assisted inference methods. The empirical method makes quick attribute judgments based on the interpretation experience accumulated over the years. The peripheral inference method is used by surveyors to judge the land types of similar surrounding objects based on known and correct land types and location characteristics. The data-assisted inference rule is that the surveyor uses various existing data to assist in the determination of the features. This study mainly uses a combination of empirical and data-assisted inference methods to carry out remote sensing measurement of the crop area. The specific methods are as follows. This research selected surveyors who have many years of experience in remote sensing interpretation of crops. After analyzing the crop structure and its distribution, national economic development level, people's living habits, and other socio-economic conditions, the surveyors quickly determine the type of land; for the patches that cannot be accurately interpreted through the existing experience, a combined analysis of each study is used. The mark database and network data are translated to assist in the interpretation to ensure the reliability and accuracy of the crop area remote sensing measurement results.

## 3 Experiments

### 3.1 Data Collection

Affected by the crop planting structure and topography of various regions, remote sensing measurement of the crop area is also difficult. To obtain more effective research conclusions, this article sets three levels of difficulty in remote sensing identification of different measurement areas according to the complexity of terrain, landforms, and planting structures, and according to these three levels, it can be collected in combination with the current stage. For the relevant data, three districts and counties, A, B, and C, were selected as the study areas. The plain area belongs to the first-class area, the B terrace area belongs to the second-class area, and the C broken area belongs to the third-class area.

### 3.2 Experimental Methods

In this paper, the combination of automatic software processing and manual verification is adopted, and the remote sensing data is first processed according to the processing flow of registration and fusion. Orthorectification includes radiometric correction, registration + fusion, mosaic, crop step, band combination and color adjustment, based on the study area, it produces two sets of orthophoto results, namely the original four-band orthophoto results and the three-band orthophoto results that simulate natural true color.

### 3.3 Accuracy Evaluation Index

The confusion matrix is a matrix of  $n$  rows and  $n$  columns, where  $n$  represents the number of categories. The confusion matrix evaluation method uses the form of a confusion matrix to display the comparison results between classification results and ground truth information. The evaluation indicators mainly include user accuracy (UA), producer accuracy, and OA.

The UA gives the prediction classification result information of a category. The formula is as follows:

$$UA = \frac{P_{nn}}{P_{qn}}. \quad (17)$$

In the formula,  $P_{nn}$  is the number of samples that are correctly classified in a certain class, and  $P_{qn}$  is the total number of classifications, i.e., the total number of rows in a confusion matrix.

$$PA = \frac{P_{nn}}{P_{pn}}. \quad (18)$$

In the formula,  $P_{nn}$  is the number of samples that are correctly classified in a certain category. OA is a statistical quantity with probabilistic meaning. It is used to give OA information. It represents the proportion of all accurately classified objects in the overall object:

$$OA = \frac{N \sum_{k=1}^i P_{kk}}{M}. \quad (19)$$

In the formula, OA is the total classification accuracy,  $i$  is the total classification category,  $M$  is the total number of samples, and  $P_{kk}$  is the number of test samples of the  $K$ 'th category.

## 4 Discussion

### 4.1 Data Fusion Technology and Remote Sensing Image

The sensors used to observe things have gradually improved their functions. When observing the physics of the earth's surface, different types of objects can reflect different electromagnetic waves. According to this phenomenon, they can be in different wavelength ranges. The objects can be distinguished from each other, as shown in Fig. 1.

Due to the complexity, diversity, and extensiveness of the research content of data fusion technology, there is no unified definition at present, and different fields have different interpretations. We analyze basic data fusion algorithms, such as Bayesian inference, fuzzy inference, cluster analysis, maximum likelihood estimation, and rough set theory, as shown in Fig. 2.

Taking into account the unique characteristics of remote sensing tile data created from a set of high definition, high resolution, data, an automatic full recovery and a one-time retrieval system are performed on the tiled area data of the remote area. The world-class remote imaging data recovery method locates all remote imaging data that intersect or relate to the composite polygon area according to the area covered by the remote imaging data. The use of cloud data storage technology has recognized the integration of multiple world-class resources, integrated large-scale data storage and management and 3D projection retrieval services, provided data support services for the production and development of common high-tech products, and served companies that need field data applications such as meteorology, transportation, region, and military services. The rate of continuous improvement of the different data integration algorithms is shown in Table 1.

The relative differences of brightness and structure are related. Analyzing factors such as different waveband ranges gives the basic situation, as shown in Table 2. The choice of neighboring pixels that are too strict or loose in similar spectra will affect the final result. If the number



**Fig. 1** Remote sensing image.

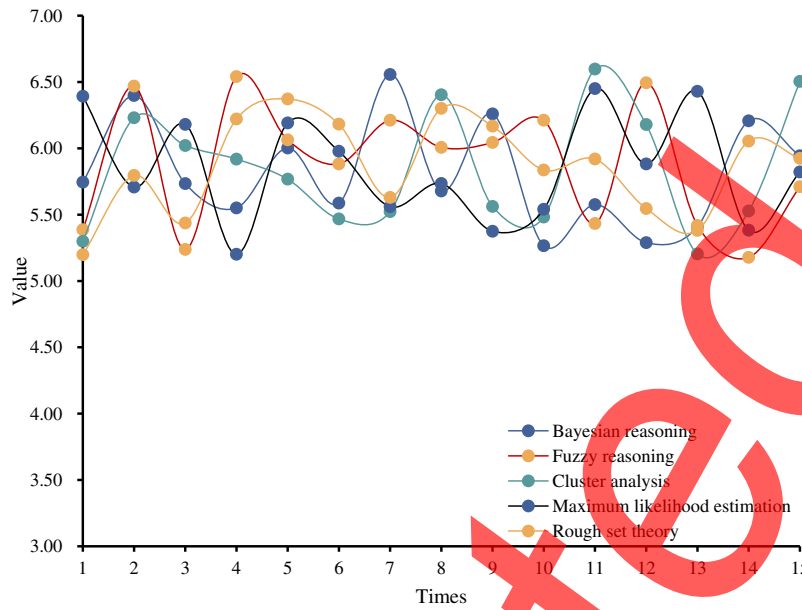


Fig. 2 Different algorithms for data fusion.

Table 1 Comparison of improving classification accuracy.

	Fuzzy reasoning	Cluster analysis	Maximum likelihood estimation
Water body	0.779	0.779	0.9
Artificial building	0.814	1	1.1
Vegetation	0.723	0.792	0.8
Soil	0.814	0.916	0.942

Table 2 Band information.

Band	Spectral range (mm)	Landsat	Spectral range (mm)
1	613 to 658	2	442 to 479
2	513 to 556	3	479 to 613
3	427 to 496	4	818 to 891
4	561 to 673	5	1620 to 1743
6	1187 to 1415	6	2103 to 2167
7	2119 to 2157	7	2249 to 2351

of adjacent spectrally similar pixels in the window range is too small, the spectral information of adjacent pixels cannot be fully utilized.

With the development of various information acquisition technologies, the signal bandwidth is getting wider and wider, and the requirements for data sampling efficiency and computer hardware are getting higher and higher. For image processing, to meet the final quality requirements of image digitization, it is necessary to design ultra-high-resolution signal acquisition

**Table 3** Data accuracy.

Fusion method	Source entropy	Correlation coefficient	Mean absolute error	Mean square error
STARFM	1.2148	0.7781	0.8231	0.2761
This research	1.4037	0.8109	0.7431	0.2205

equipment, which greatly increases the cost of high-precision signals and processing. The degree of preservation of image spectral information is usually expressed by the degree of spectral distortion. Generally speaking, for the same image, the greater the value of the spectral distortion is, the worse the spectral retention is, and the more serious the spectral distortion is compared with the original multispectral image. The data measurement accuracy analysis of this section is shown in Table 3.

## 4.2 Comparative Analysis of Crop Extraction Area and Measurement Time

### 4.2.1 Analysis of crop extraction area

Checking the data, we can see that wheat, cotton, and corn are the main types in area A, with more cotton in the northwest; wheat is the main type in area B; and cotton and corn are more in central area C. Taking into account the lack of basic statistical data in each region, this paper intends to use visual interpretation methods to use artificial digitized results to evaluate the wheat, corn, and cotton planting area results extracted by the two methods used in this paper. The extraction results of the crop extraction area are shown in Fig. 3.

It can be seen from Fig. 3 that, although the results extracted by different methods are different, the overall distribution of the results extracted by different methods is roughly equivalent and consistent with the trend in the data. Among them, the largest planting area in areas A and B is wheat, which are 43,507.3 and 13,285.38 m<sup>2</sup>, respectively, and the largest planting area in area C is 79,765.4 m<sup>2</sup> of corn.

### 4.2.2 Comparative analysis of measurement time

This article compares the object-oriented automatic measurement speed of each research area with the average manual processing speed of operators with rich experience in measuring crop area. In the ArcGIS software platform, it takes the average time to check and modify nine types of speckle types screen by screen and segment the oversized speckles. Comparative analysis of measurement time is shown in Table 4 and Fig. 4.

**Fig. 3** Extraction results of crop extraction area.

**Table 4** Comparative analysis of measurement time.

Research object		Object-oriented taxonomy processing time			
Types	Area (km <sup>2</sup> )	Manual processing time (days)	Software processing time (days)	Manual modification time (days)	Subtotal
A plain area	874	28	1.5	6	7.5
B terraces	384	12	0.5	3	3.5
C broken area	199	9	0.5	2	2.5
Total	1457	49	2.5	11	13.5

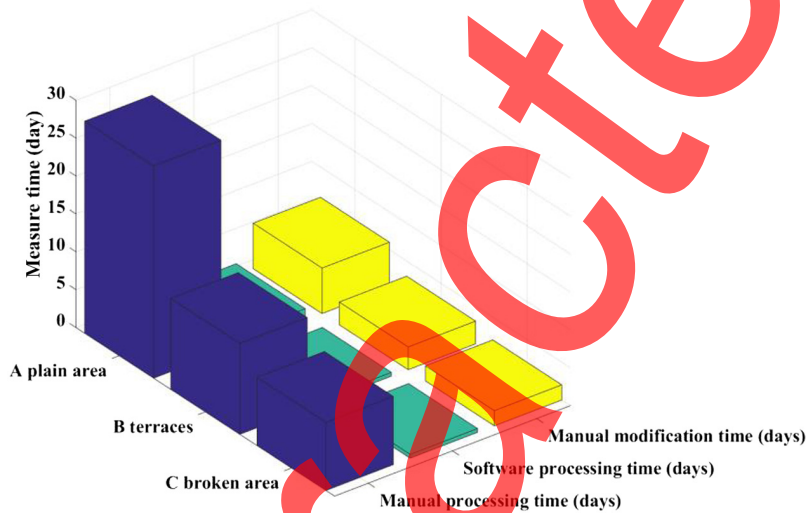


**Fig. 4** Comparative analysis of measurement time.

From Table 4 and Fig. 4, it can be seen that the object area-oriented automatic measurement method for crop area remote sensing measurement in the plain area is 3.2 times the speed of manual visual interpretation. The automatic speed measurement area of the object-oriented platform is 2.6 times that of the manual visual measurement speed. The object-oriented automatic measurement speed of the broken area is 2.5 times that of the manual visual measurement speed. In addition, from the object-oriented automatic measurement experiment, it can be found that the software processing time does not increase linearly with the measurement area, and the software processing can be performed by multiple threads simultaneously. In other words, the larger the measurement area is, the more object-oriented it is. The advantages of the automatic measurement method over the manual measurement method are more obvious, as shown in Table 5.

**Table 5** Result accuracy data.

Related data	Convolutional neural network	Algorithm
New source entropy	1.1159	1.2145
Correlation coefficient	0.6701	0.4358
Mean absolute error	0.7829	0.6956
Mean square error	0.2157	0.1847

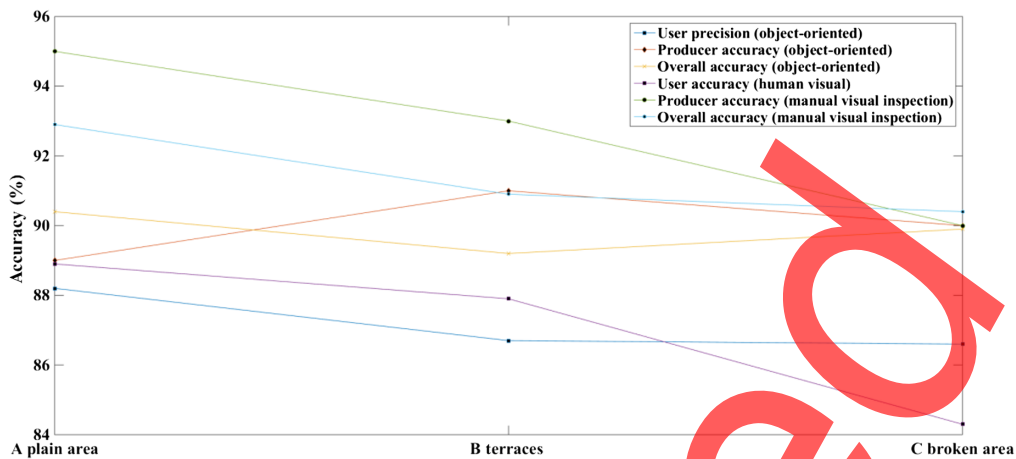


Fig. 5 Classification accuracy analysis.

### 4.3 Comparative Analysis of Measurement Accuracy

#### 4.3.1 Analysis of area and classification accuracy

This study uses the confusion matrix evaluation method, making full use of field sampling survey data and randomly selecting 100 inspection samples by type from the field vector survey spot. When the number of inspection samples is  $<100$ , the spectrum and texture of the inspection samples is analyzed. The time-equivalent characteristics are used to establish sample interpretation marks, and a number of inspection points are selected to make up 100; if it is still not possible to complete, all of the spots that are consistent with the interpretation marks of such samples are used as inspection points. Through the spatial connection method, one-to-one correspondence is made between the classification type of the inspection point and the field survey type, and then the measurement accuracy is evaluated by constructing a confusion matrix. The classification accuracy analysis is shown in Fig. 5.

As can be seen from Table 4, the area accuracy of the plain area A is 95.3%, the area accuracy of the terrace area B is 93.5%, and the area accuracy of the broken area C is 92.6%. The classification accuracy of the remote sensing measurement of crop area using an object-oriented automatic measurement method, including UA and artificial visual measurement, is basically the same; producer accuracy and OA are slightly lower than manual visual interpretation methods, but both can reach more than 90%.

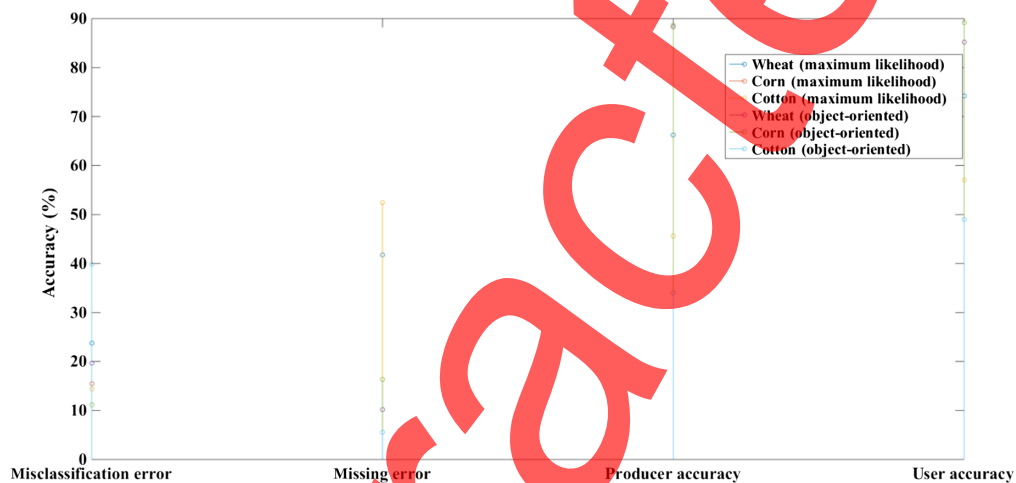
#### 4.3.2 Comparison of maximum likelihood and object-oriented accuracy

Maximum likelihood classification is one of the more important algorithms in supervised classification. It is widely used in various systems. The principle of the main calculation process can be roughly divided into five parts: (1) the number of classification features of the study area is determined according to the spectral characteristics of the image; (2) according to the basic ground conditions of the research area that is mastered, the training area of the classification target is selected, and the basis is determined. The prior probability obtained in this training area; (3) the pixels of each class in the training area are sequentially substituted into the entire image, and the maximum value generated when they are sequentially substituted is used as the category in the image pixel; (4) for the entire image, a value for each category is specified, the classified pixel value is replaced with the category value, and then different colors are assigned to each category to output it to get the classified image that we need; and (5) check the accuracy of the classification result. There are too many missing points, and the above four processes need to be repeated until the results obtained are satisfactory. This is shown in Table 6 and Fig. 6.

From Table 6 and Fig. 6, we can see that, although the maximum probability distribution is more accurate than the correlation coefficient when measuring grains, the inaccurate error and

**Table 6** Results of maximum likelihood classification and object-oriented classification.

Classification	Maximum likelihood classification			Object-oriented classification		
	Wheat	Corn	Cotton	Wheat	Corn	Cotton
Category						
Misclassification error (%)	23.82	15.42	14.38	19.67	11.11	39.78
Missing error (%)	41.78	52.39	52.39	10.19	16.34	5.51
Producer accuracy (%)	66.22	45.61	45.61	88.34	88.65	33.98
UA (%)	74.18	57.06	57.06	85.23	89.23	48.97
OA (%)		66.48			89.11	
Kappa coefficient		0.61			0.89	

**Fig. 6** Results of maximum likelihood classification and object-oriented classification.

the missing error are greater than the relative coefficient. The average adjustment rates were 66.48% and 89.11%, respectively.

## 5 Conclusions

1. In this paper, three methods of object-oriented classification, artificial visual interpretation, and maximum likelihood classification, which excel in the classification of current status of land use, are selected. When it is necessary to quickly obtain the remote sensing measurement results of large-scale crop areas, the use of the object-oriented computer automatic classification method is a better choice.
2. Although this paper is limited by the lack of multiphase data collection of high-resolution remote sensing images, through sufficient comparison and analysis of satellite image data in multiple phases, such as before planting, vigorous growth, and post-harvest, combined with phenological data, a remote sensing measurement of crop area was completed on the basis of single-phase high-resolution image data.
3. In this article, the object-oriented automatic measurement method is described as the accuracy after manual modification and after automatic extraction by the computer. The accuracy before modification varies from 60% to 80% according to the operating area and image quality. It fully meets the needs of applications. In the future, we will further research pure computer automatic classification to further improve its accuracy.

4. The image fusion process adopts the blocking theory, which reduces the memory footprint during the operation of the algorithm and reduces the demand for computer hardware for program operation; in addition, the particle swarm optimization algorithm obtains the fusion coefficient, which solves the problem of traditional experience value fusion. The problem is that the fusion coefficient cannot adapt to the changes in the data to be fused.

## Acknowledgments

No funding was used to support this study. There are no potential competing interests in our paper. All authors have seen and approved the manuscript to submit to the journal. We confirm that the content of the manuscript has not been published or submitted for publication elsewhere.

## Code, Data, and Materials Availability

This article does not cover data research. No data were used to support this study.

## References

1. C. Gong, J. Han, and X. Lu, "Remote sensing image scene classification: benchmark and state of the art," *Proc. IEEE* **105**(10), 1865–1883 (2017).
2. K. Karalas, G. Tsagkatakis, and M. Zervakis, "Land classification using remotely sensed data: going multilabel," *IEEE Trans. Geosci. Remote Sens.* **54**(6), 3548–3563 (2016).
3. W. H. Su et al., "Land use and land cover change in Vientiane area, Lao PDR using Object-Oriented classification on multitemporal landsat data," *Adv. Sci. Lett.* **23**(11), 11340–11344 (2017).
4. B. Demir and L. Bruzzone, "Hashing-based scalable remote sensing image search and retrieval in large archives," *IEEE Trans. Geosci. Remote Sens.* **54**(2), 892–904 (2015).
5. Y. Pan et al., "FDPPGAN: remote sensing image fusion based on deep perceptual patchGAN," *Neural Comput. Appl.* **33**, 9589–9605 (2021).
6. H. He et al., "Remote sensing image super-resolution using deep–shallow cascaded convolutional neural networks," *Sens. Rev.* **39**(5), 629–635 (2019).
7. P. Pahlavani and B. A. Bigdeli, "Mutual information-Dempster–Shafer based decision ensemble system for land cover classification of hyperspectral data," *Front. Earth Sci.* **11**(4), 774–783 (2017).
8. D. Osaku et al., "Fine-tuning contextual-based optimum-path forest for land-cover classification," *IEEE Geosci. Remote Sens. Lett.* **13**(5), 735–739 (2016).
9. P. P. Joao, P. P. Luciene, and R. P. Danillo, "A hyperheuristic approach for unsupervised land-cover classification," *IEEE J. Sel. Top. Appl. Earth Obs. Remote Sens.* **9**(6), 2333–2342 (2016).
10. S. J. Peter et al., "Fine resolution probabilistic land cover classification of landscapes in the Southeastern United States," *Int. J. Geo-Inf.* **7**(3), 107 (2018).
11. F. Daumard et al., "Measurement and correction of atmospheric effects at different altitudes for remote sensing of sun-induced fluorescence in oxygen absorption bands," *IEEE Trans. Geosci. Remote Sens.* **53**(9), 5180–5196 (2015).
12. H. Y. Xu, W. F. Zhou, and J. I. Shi-Jian, "Review of estimation on oceanic primary productivity by using remote sensing methods," *J. Appl. Ecol.* **27**(9), 3042–3050 (2016).
13. G. Y. Wang, D. Q. Zhou, and Y. Zhao, "Data analysis of micro vibration on orbit measurement for remote sensing satellite," *J. Astronaut.* **36**(3), 261–267 (2015).

**Kexue Liu** received his doctoral degree in land planning from South China Agricultural University in 2015. Currently, he is an associate professor at Xinhua College, Sun Yat-sen University. His research interests include resources and urban planning.

**Lingyu Xia** received her master's degree in land planning from Hua Zhong Agricultural University in 2015. Currently, she is a lecturer at Xinhua College, Sun Yat-sen University. Her research interests include resources and urban planning.

**DongYa Zhu** received his master's degree in land planning from South China Agricultural University in 2013. Currently, he is a chief engineer at Guangdong Dong Tu Planning Technology Co., Ltd. His research interests include resources and land planning.

**Jianbo Xu** received his doctoral degree in GIS from South China Agricultural University in 2008. Currently, he is a professor at the College of Resource and Environment, South China Agricultural University. His research interests include GIS and remote sensing image recognition.

Retracted